JOURNAL OF MATERIALS SCIENCE 24 (1989) 220–226

Microstructure development in SnO_2 with and without additives

TOSHIO KIMURA, SHUSUKE INADA, TAKASHI YAMAGUCHI
Faculty of Science and Technology, Keio University, 3-14-1 Hiyoshi, Kohoku-ku, Yokohama 223, Japan

The microstructure development in pure and ZnO-, Nb_2O_5- or (ZnO + Nb_2O_5)-containing SnO_2 has been studied. Sintering of pure SnO_2 proceeds by an evaporation–condensation mechanism and grain and pore sizes increase without densification. The pores are open with no closed pores developed. Grain and pore structures become homogeneous with sintering time. Sintered pure SnO_2 is porous and has large grains. Nb_2O_5 suppresses particle coarsening and pore growth but does not promote densification, leading to porous sintered bodies with small grains. ZnO and (ZnO + Nb_2O_5) promote densification but do not suppress particle and grain coarsening. The sintered body is composed of large grains with pores located on grain boundaries.

1. Introduction

The microstructure of a sintered body is determined by two processes, densification and particle coarsening [1]. Bulk or grain-boundary diffusion is the main mechanism for densification. When these mechanisms are predominant during sintering, high-density products with small grains will be expected. Surface diffusion or evaporation–condensation results in particle coarsening. When either one of these mechanisms is predominant, densification does not occur and a high density is hardly attained. Usually densification and particle coarsening occur simultaneously. Furthermore, the relative contribution of material transport mechanisms depends on the sintering conditions and powder characteristics. This complexity in sintering phenomena makes the control of microstructure difficult.

The sintering of pure stannic oxide (SnO_2) occurs mainly by the evaporation–condensation mechanism [2]. Shrinkage is small and grain and pore sizes increase during sintering [3, 4]. Additives such as ZnO, CuO and MnO_2, enhance densification [5, 6]. Although the mechanisms of enhancing densification have not been investigated thoroughly, it is at least evident that these additives promote bulk and/or grain-boundary diffusion or form a liquid phase. The study of microstructure development in SnO_2 with additives will elucidate the effect of material transport mechanisms on the microstructure. This paper deals with the microstructure development in SnO_2 with and without additives. ZnO and Nb_2O_5 were selected as additives [7–9].

2. Experimental procedure

Two kinds of SnO_2 powder were used; one was commercial (SnO_2 I) and the other was prepared in our laboratory (SnO_2 II). The latter was prepared by the following procedure. One mole of $SnCl_2 \cdot 2H_2O$ was dissolved into 1 dm^3 of 12 N HCl and poured into 1 dm^3 of $(NH_4)_2C_2O_4$ aqueous solution (1 mol dm^{-3}). The dried precipitate, SnC_2O_4, was fired at 300° C for 10 h and then 700° C for 10 h in O_2. The SnO_2 obtained was mixed with water and deagglomerated with a homogenizer for 30 min. An SEM photograph of the product is shown in Fig. 1, together with that of commercial SnO_2. The SnO_2 II powder, which was used to study the additive effect, had a narrow particle size distribution with an average particle size of about 0.2 μm. The SnO_2 I powder had a broad particle size distribution. ZnO and Nb_2O_5 were added to SnO_2 separately or simultaneously in a ball mill for 19 h using ethanol as a medium. The same weights of ZnO and Nb_2O_5 were mixed when both were added simultaneously.

The powders were pressed into cylinders of 2.7 mm height and 11 mm diameter under a pressure of 98 MPa using a polyvinyl alcohol solution (10 wt %) as a binder. The binder was burnt out at 500° C for 16 h. The sintering behaviour was examined between 1000° C and 1300° C at 100° C intervals. The green compact was placed in a furnace at the desired temperature and heated for the desired time period in air. The compact was then withdrawn from the furnace and cooled in air.

The microstructure was examined by scanning electron microscopy (SEM) and mercury porosimetry. Density was determined by measuring the weight and dimensions of the compact. Total pore volume was calculated from the density, and open pore volume was obtained by porosimetry. Densities of 6993, 5780, 4550 and 5820 kg m^{-3} for SnO_2, ZnO, Nb_2O_5 and $3ZnO \cdot Nb_2O_5$, respectively, were used to calculate the theoretical density and total pore volume. Phases were identified by X-ray diffraction analysis using Cu$K\alpha$ radiation. Lattice parameters were calculated from d_{211} and d_{220}.

0022–2461/89 $03.00 + .12

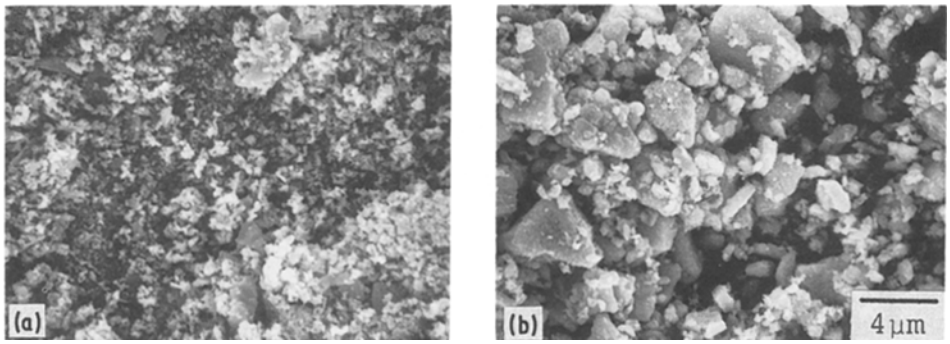

Figure 1 SEM photographs of (a) SnO_2 II and (b) SnO_2 I.

3. Results and discussion

3.1. Microstructure development in pure SnO_2

Figs 2 and 3 show the SEM photographs and porosimetry curves of SnO_2 II sintered at various temperatures for 3 h. The grain size increased with increasing sintering temperature. The open pore volume was practically constant but the pore size increased as the temperature increased. The increase in pore size is also observed from the SEM photographs (Fig. 2). Table I shows the density and total and open pore volumes. The density was practically constant. The measured open pore volumes were larger than the total pore volumes by 1 to 2%. Since the error of 1% in density determination results in an error of 2% in total pore volume, the total pore volume is practically equal to the open pore volume, indicating that all pores were open and that no closed pore was formed during sintering.

The effect of the particle size distribution on microstructure development was examined for SnO_2 I. Fig. 4 shows SEM photographs of SnO_2 I sintered at various temperatures for 1 h. The surface of large particles was rather smooth in the as-received state (Fig. 1b) but small particles evolved on the surface of large particles when fired above 1000° C, indicating that the large particles had been in an aggregated state. Pores were visible at the surface of large particles. The particle size distribution narrowed as the sintering temperature increased.

Fig. 5 shows porosimetry curves and in Table II are shown density and total and open pore volumes for the green and sintered SnO_2 I compacts. The density was practically constant for green and sintered compacts. The open pore volume was smaller in the green compact than in the sintered compacts. From Table II about 35% of the total pore volume in green compacts was closed. These closed pores were located in aggregates of starting SnO_2 I particles, but became open on firing. The increase in the volume of pores with a radius of about 0.03 μm in the 1000° C curve supports this view. Above 1000° C the total pore volume is practically equal to the open pore volume. The pore size distribution for the compact sintered at 1000° C was broad, and the distribution narrowed with an increase in temperature. These results indicate that homogenization of microstructure occurred during sintering.

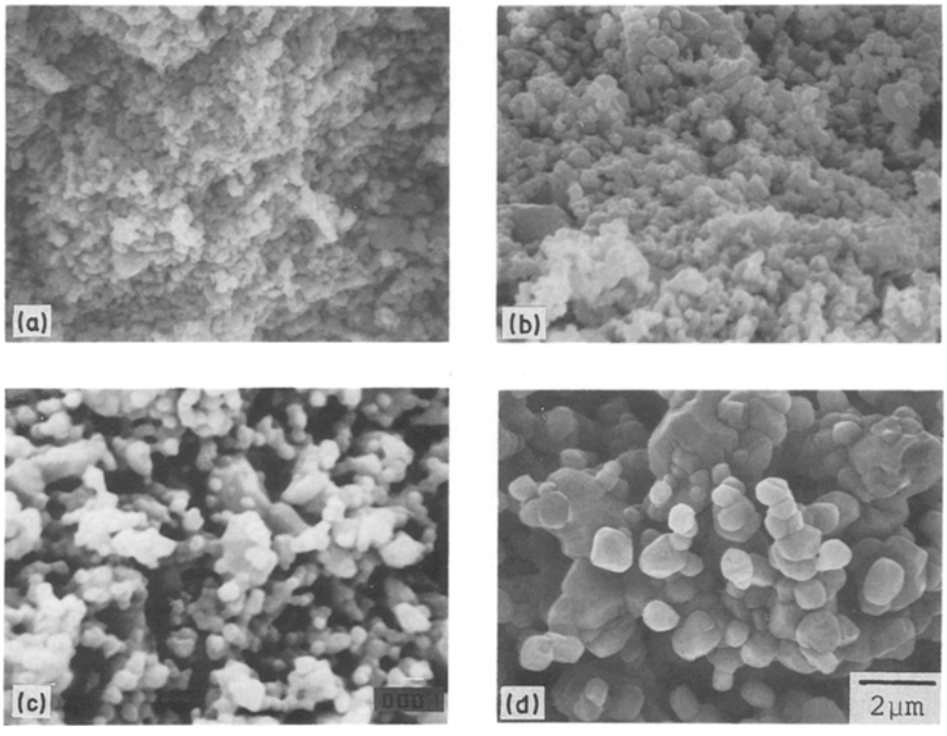

Figure 2 SEM photographs of fracture surfaces of SnO_2 II sintered for 3 h at (a) 1000° C, (b) 1100° C, (c) 1200° C and (d) 1300° C.

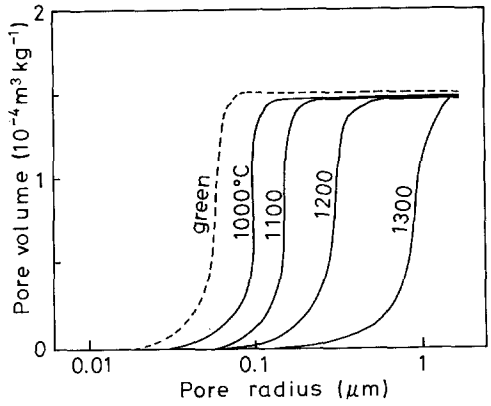

Figure 3 Porosimetry curves of SnO_2 II sintered for 3 h at various temperatures. The broken line is for the green compact.

The sintering characteristics of pure SnO_2 are summarized as follows. Shrinkage during sintering is small and the density is practically constant in the temperature range studied. Grain and pore sizes increase as sintering proceeds. Pores are open during sintering and no closed pores are formed during sintering. Microstructure becomes homogeneous with sharp distributions of grain and pore size. These characteristics may be observed in any system in which evaporation–condensation is the predominant mechanism for sintering [3, 10, 11].

3.2. Phase relations and densification of SnO_2 with additives

Samples with additives were fired for 3 h between 1000° C and 1300° C at 100° C intervals. No diffraction peaks other than those of SnO_2 were detected for samples with up to 3 wt % of total additives. Samples with more than 5 wt % ZnO or Nb_2O_5 contained ZnO and $ZnSnO_3$ or Nb_2O_5 and $SnNb_2O_6$, respectively, and those with more than 5 wt % (ZnO + Nb_2O_5) contained $3ZnO \cdot Nb_2O_5$, ZnO and $ZnSnO_3$. Table III shows the phases detected by X-ray diffraction analysis excluding SnO_2. This result indicates that the samples are not in equilibrium when fired for 3 h. The lattice parameters of all samples, with and without additives, were practically constant (d_{211} = 0.1764 ± 0.0001 nm, d_{220} = 0.1674 ± 0.0001 nm). Nb_2O_5 is reported not to change the lattice parameters within experimental error [9]. Since the detection limit by X-ray diffraction analysis was a few per cent, it is difficult to measure the solubility limit of additives in SnO_2. The theoretical density and total pore volume were calculated assuming no solubilities of ZnO and Nb_2O_5 in SnO_2 and no compound formation other than $3ZnO \cdot Nb_2O_5$.

TABLE I Density and total and open pore volumes for green and sintered SnO_2 II

Temperature (° C)	Density		Pore volume (10^{-6} m^3 kg^{-1})	
	kg m^{-3}	% theoretical	Total	Open
(green)	3480	49.8	144.4	146.9
1000	3485	49.8	143.9	146.0
1100	3487	49.9	143.8	146.9
1200	3478	49.7	144.5	146.1
1300	3485	49.8	143.9	146.8

Fig. 6 shows the density of sintered compacts as a function of temperature and additive content. The addition of ZnO and (ZnO + Nb_2O_5) enhanced densification but the effect of Nb_2O_5 on the densification was small. Excessive amounts of ZnO and (ZnO + Nb_2O_5) decreased the density. Second solid phase particles cause stresses and retard densification [12]. This effect is enhanced by an increase in the volume fraction of the second phase. It is possible that an excessive amount of ZnO, $ZnSnO_3$ and $3ZnO \cdot Nb_2O_5$ decreased the density by this inclusion effect. Os'kina *et al.* [7] reported that ZnO and (ZnO + Nb_2O_5) enhanced the densification of SnO_2 and that Nb_2O_5

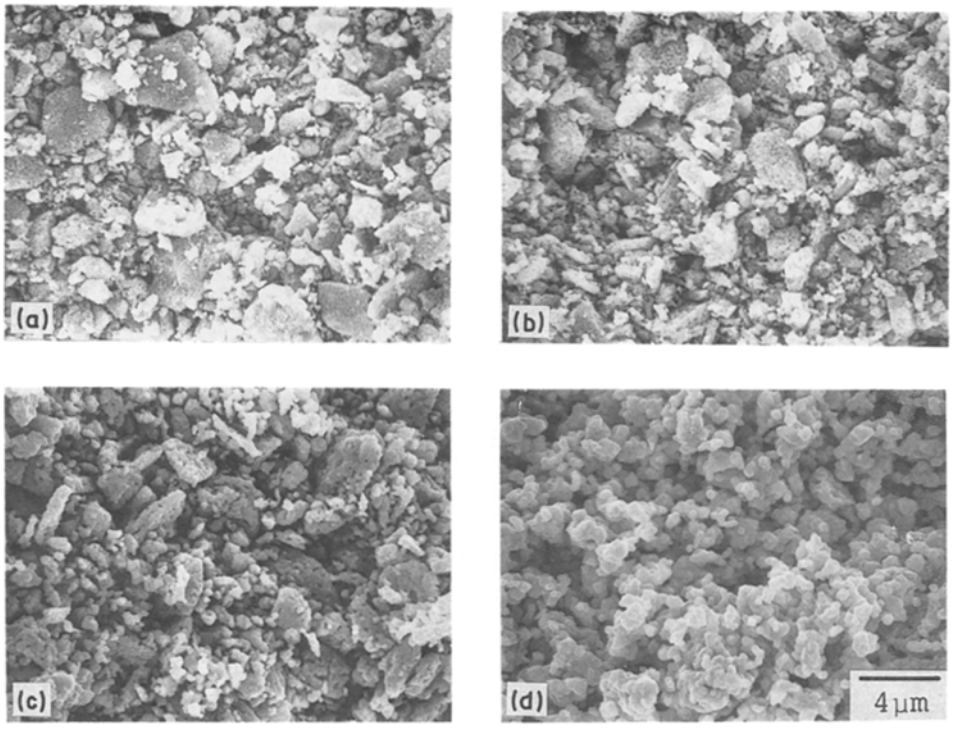

Figure 4 SEM photographs of fracture surfaces of SnO_2 I sintered for 1 h at (a) 1000° C, (b) 1100° C, (c) 1200° C and (d) 1300° C.

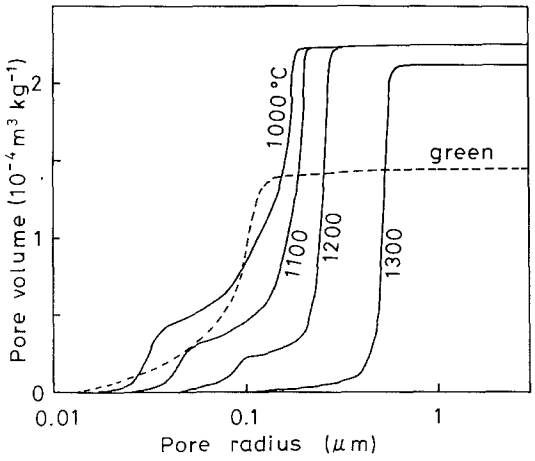

Figure 5 Porosimetry curves of SnO_2 I sintered for 1 h at various temperatures. The broken line is for the green compact.

had little effect below 1300° C, which agrees with the present results. Takahashi *et al.* [9] reported that SnO_2 with more than 3 wt % Nb_2O_5 had a density about 75% of theoretical at 1300° C. The powder characteristics would give a difference in densification behaviour between the present experiments and those of Takahashi *et al.*

3.3. Grain and pore structures of SnO_2 with additives

Fig. 7 shows the microstructures of samples containing a total of 3 wt % additives sintered between 1000 and 1300° C. Microstructure developments for other additive contents were almost the same as those with 3 wt % additive. When ZnO and (ZnO + Nb_2O_5) were added, grain sizes were almost the same as those of pure SnO_2 at 1000 and 1100° C, and larger at 1200 and 1300° C than those of pure SnO_2. The latter additive gave a larger grain size than the former one. Facets (grain boundaries) between grains developed above 1200° C. Nb_2O_5 suppressed grain growth as compared with pure SnO_2. The grain size increased slightly as the temperature increased.

Fig. 8 shows the porosimetry curves for samples with 3 wt % additives. When ZnO and (ZnO + Nb_2O_5) were added, the open pore volume decreased as the temperature increased. The observed decrease in open pore volume is related to densification (decrease in total pore volume) and to closed pore formation. The total pore volume is plotted at the right-hand side of each figure. Closed pores formed above 1200 and 1100° C for ZnO and (ZnO + Nb_2O_5), respectively. Pore size increased as the temperature increased, but the degree of pore growth was smaller than that in pure SnO_2 (Fig. 2).

TABLE II Density and total and open pore volumes for green and sintered SnO_2 I

Temperature (° C)	Density		Pore volume (10^{-6} m^3 kg^{-1})	
	kg m^{-3}	% theoretical	Total	Open
(green)	2726	39.0	223.8	145.8
1000	2732	39.1	223.0	225.5
1100	2727	39.0	223.7	225.0
1200	2730	39.0	223.3	225.5
1300	2839	40.6	209.2	212.8

When Nb_2O_5 was added, the open pore volume decreased slightly and no closed pores formed. The pore size increased with increasing temperature but the size was smaller than that in pure SnO_2. As pore size was closely related to grain size, suppression of grain growth resulted in the suppression of pore growth. Nb_2O_5 would reduce the evaporation–condensation rate of SnO_2, but further study is necessary to elucidate the suppressing mechanism in grain growth.

3.4. Microstructure development of SnO_2 with ZnO or (ZnO + Nb_2O_5)

Paria *et al.* [5] deduced grain-boundary diffusion as the predominant densification mechanism in the SnO_2–ZnO system, based on the isothermal shrinkage data. As extensive particle coarsening and grain growth occurred during sintering in this system as shown in Fig. 7, the densification mechanism cannot be determined simply from the isothermal shrinkage data. Since the addition of ZnO and (ZnO + Nb_2O_5) enhanced densification, it is at least evident that materials are transported by bulk and/or grain-boundary diffusion.

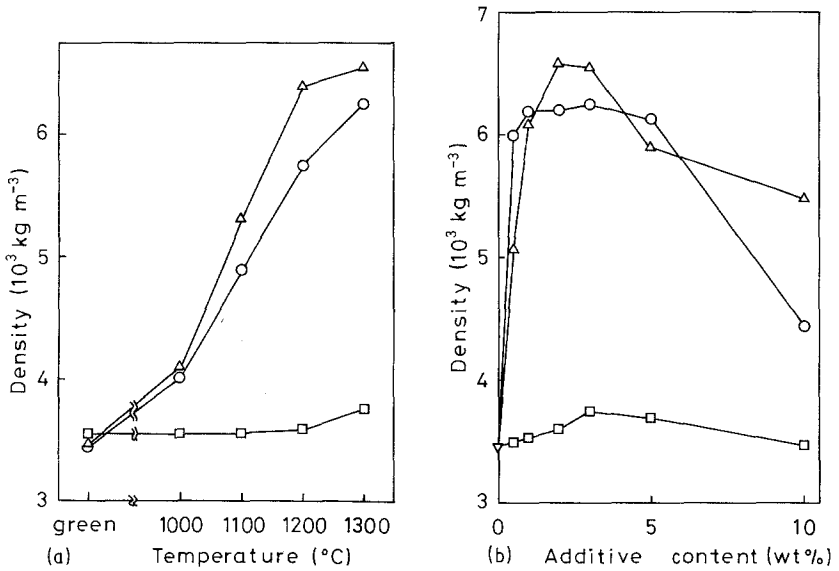

Figure 6 (a) The temperature dependence of the density of sintered SnO_2 with 3 wt % additives and (b) the effect of additive content on the density of SnO_2 sintered at 1300° C for 3 h. Additive (○) ZnO, (△) ZnO + Nb_2O_5, (□) Nb_2O_5.

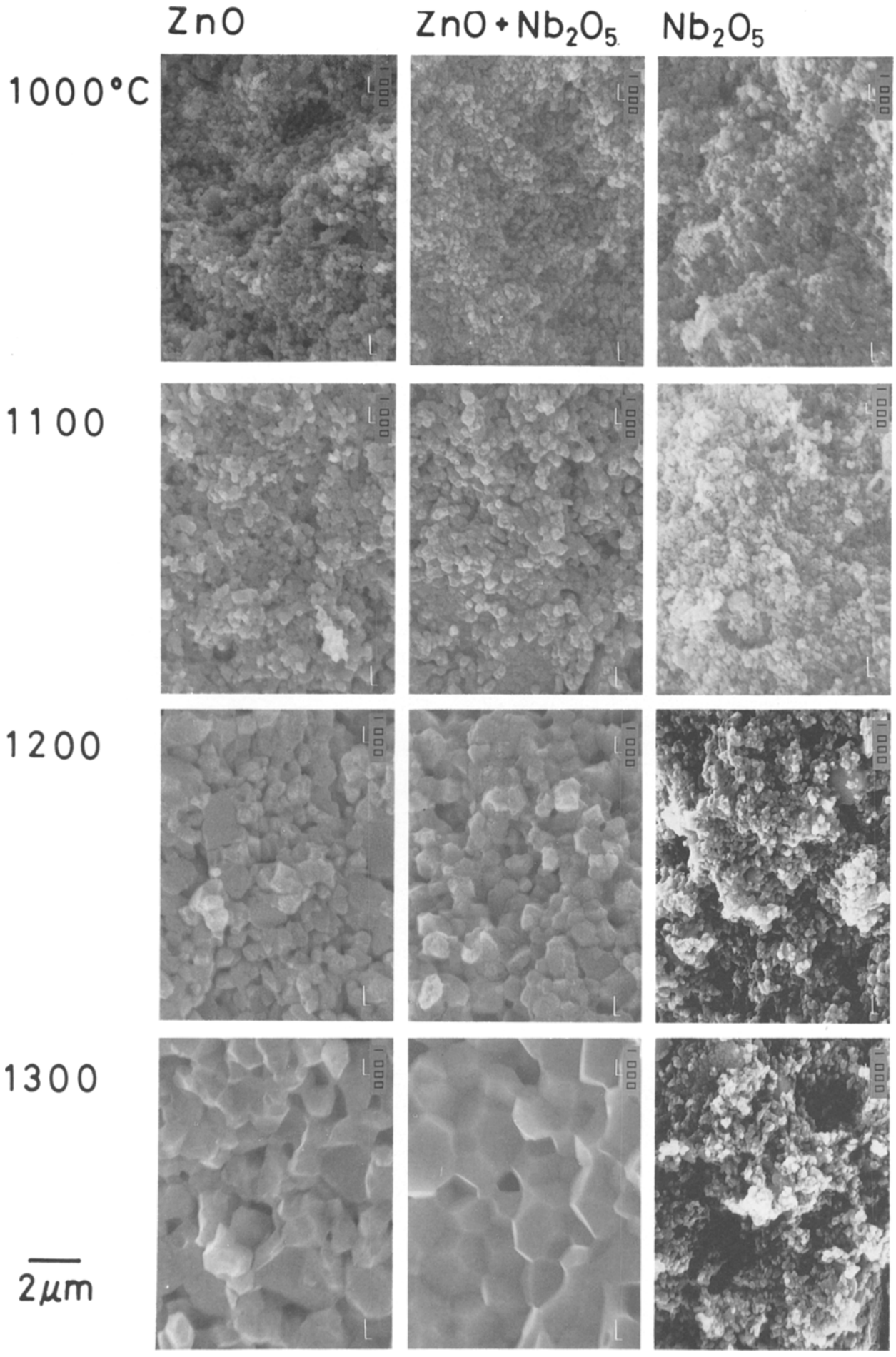

Figure 7 Microstructure development of SnO_2 II with 3 wt % additives sintered at various temperatures for 3 h.

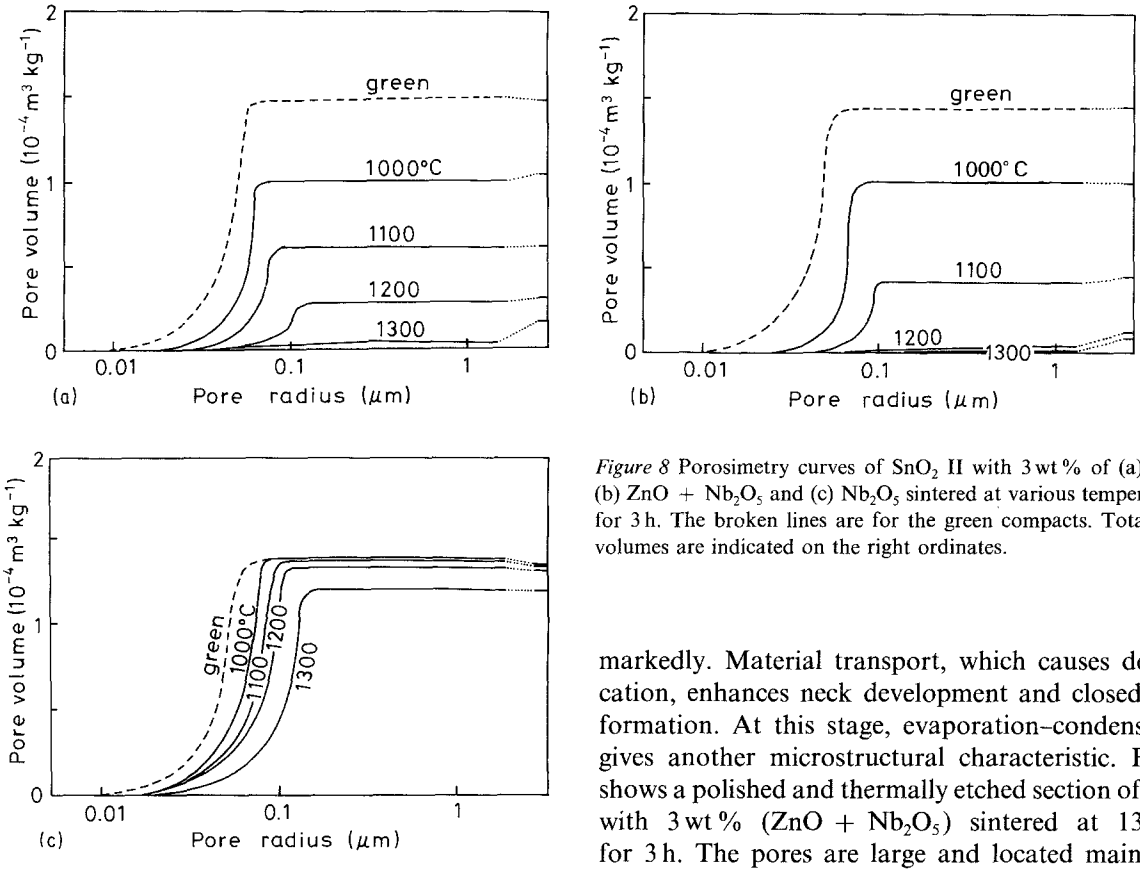

Figure 8 Porosimetry curves of SnO_2 II with 3 wt % of (a) ZnO, (b) ZnO + Nb_2O_5 and (c) Nb_2O_5 sintered at various temperatures for 3 h. The broken lines are for the green compacts. Total pore volumes are indicated on the right ordinates.

However, the operative mechanism has not been fully understood.

When ZnO or (ZnO + Nb_2O_5) was added, particle coarsening during the initial stage of sintering (at 1000 and 1100° C) occurred along with densification (Fig. 7). Thus, ZnO enhances material transport by bulk and/or grain-boundary diffusion but does not suppress evaporation–condensation. When Nb_2O_5 is present alone, particle coarsening is suppressed but not in the coexistence of ZnO. The formation of $3ZnO \cdot Nb_2O_5$ is a possible reason.

When particle coarsening occurs without densification as in pure SnO_2, the pores grow. When densification takes place along with particle coarsening, the rate of pore growth decreases, since the total pore volume is decreased. Whittemore and Sipe [13] found that pore growth is small in α-Al_2O_3 but large in γ-Al_2O_3, MgO and Fe_2O_3, and postulated the following mechanisms of pore growth: particle coarsening by surface diffusion and evaporation–condensation, particle coalescence and phase transformation. In the present systems, evaporation–condensation is a possible mechanism or pore growth.

At 1200 and 1300° C, grain boundaries developed markedly. Material transport, which causes densification, enhances neck development and closed pore formation. At this stage, evaporation–condensation gives another microstructural characteristic. Fig. 9 shows a polished and thermally etched section of SnO_2 with 3 wt % (ZnO + Nb_2O_5) sintered at 1300° C for 3 h. The pores are large and located mainly on grain boundaries. Pores are grown by coalescence associated with grain growth during the final stage of sintering [14]. Usually the increase in pore size results in a decrease in pore mobility and the formation of intragrain pores [15]. In the present system, pores can move readily by evaporation–condensation, resulting in a slow breakaway from grain boundaries and also in large pores on grain boundaries.

4. Conclusions

The sintering of pure SnO_2 occurs predominantly by evaporation–condensation. The grain size increases as sintering proceeds, resulting in pore growth. The pores are open during the sintering and microstructure becomes homogeneous. Addition of Nb_2O_5 reduces the material transport rate by evaporation–condensation, and suppresses the particle coarsening and pore growth. Densification is not enhanced significantly by Nb_2O_5. Addition of ZnO and (ZnO + Nb_2O_5) enhances material transport leading to densification (bulk and/or grain-boundary diffusion) but does not suppress evaporation–condensation. Particle coarsening occurs during the initial stage and large pores on grain boundaries are formed during the final stage of sintering.

TABLE III Phases other than SnO_2 in sintered SnO_2 II with additives

Temperature (° C)	Additive and content (wt %)					
	ZnO		ZnO + Nb_2O_5		Nb_2O_5	
	5	10	5	10	5	10
(green)	–	ZnO	–	ZnO	–	Nb_2O_5
1000	$ZnSnO_3$, ZnO	$ZnSnO_3$, ZnO	$3ZnO \cdot Nb_2O_5$	ZnO, $ZnSnO_3$, $3ZnO \cdot Nb_2O_5$	–	Nb_2O_5
1100	$ZnSnO_3$, ZnO	$ZnSnO_3$, ZnO	$3ZnO \cdot Nb_2O_5$	ZnO, $ZnSnO_3$, $3ZnO \cdot Nb_2O_5$	–	Nb_2O_5
1200	$ZnSnO_3$, ZnO	$ZnSnO_3$	$3ZnO \cdot Nb_2O_5$	ZnO, $ZnSnO_3$, $3ZnO \cdot Nb_2O_5$	–	$SnNb_2O_6$
1300	$ZnSnO_3$, ZnO	$ZnSnO_3$	$3ZnO \cdot Nb_2O_5$	ZnO, $ZnSnO_3$, $3ZnO \cdot Nb_2O_5$	–	$SnNb_2O_6$

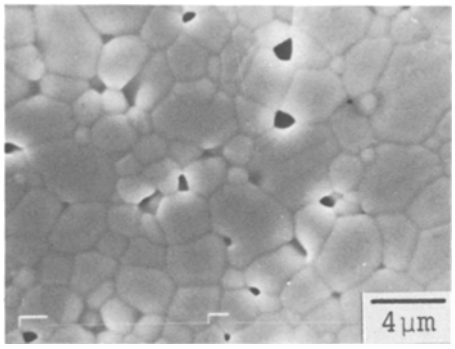

Figure 9 Microstructure of polished and thermally etched section of SnO_2 with 3 wt % ZnO + Nb_2O_5 sintered at 1300° C for 3 h.

Acknowledgements

The authors are grateful to Mr A. Yamamoto for a preliminary experiment and to Mr K. Oeda of Nihon Kagaku Sangyo Co. Ltd for supplying SnO_2 powder.

References

1. D. L. JOHNSON, *Mater. Sci. Res.* **11** (1978) 137.
2. S. J. PARK, K. HIROTA and H. YAMAMURA, *Ceram. Internat.* **10** (1984) 116.
3. T. QUADIR and D. W. READY, *Mater. Sci. Res.* **16** (1984) 159.
4. O. J. WHITTEMORE and J. A. VARELA, *ibid.* **13** (1980) 51.
5. M. K. PARIA, S. BASU and A. PAUL, *Trans. Indian Ceram. Soc.* **42** (1983) 90.
6. P. H. DUVIGNEAUD and D. REINHARD, *Sci. Ceram.* **12** (1984) 287.
7. T. E. OS'KINA, K. B. ZABORENKO, I. G. MEL'NIKOVA and T. I. PRON'KINA, *Steklo Keram.* **12** (1982) 21.
8. T. E. OS'KINA, T. I. PRON'KINA, K. B. ZABORENKO and I. G. MEL'NIKOVA, *Vestn. Mosk. Univ. Ser. 2: Khim.* **25** (1984) 51.
9. J. TAKAHASHI, I. YAMAI and H. SAITO, *Yogyo Kyokai Shi* **83** (1975) 362.
10. D. W. READY, J. LEE and T. QUADIR, *Mater. Sci. Res.* **16** (1984) 115.
11. J. LEE and D. W. READY, *Mater. Sci. Res.* **16** (1984) 145.
12. L. C. De JONGHE and R. K. BORDIA, *Acta Metall.* **32** (1984) 1003.
13. O. J. WHITTEMORE Jr and J. J. SIPE, *Powder Technol.* **9** (1974) 159.
14. W. D. KINGERY and B. FRANCOIS, in "Sintering and Related Phenomena", edited by G. C. Kuczynski, N. A. Hooton and C. F. Gibbon (Gordon and Breach, New York, 1967) p. 471.
15. R. J. BROOK, *Treatise Mater. Sci. Technol.* **9** (1976) 331.

Received 11 December 1987
and accepted 6 May 1988